Evolution of self-organized bulk vortex structure induced by hole doping in the high-temperature superconductor $YBa_2Cu_3O_{7-\delta}$

A. I. Mansour,* Rongchao Ma, M. Egilmez, M. M. Saber, I. Fan, K. H. Chow, and J. Jung†
Department of Physics, University of Alberta, Edmonton, Alberta, Canada T6G 2G7
(Received 9 April 2009; published 22 May 2009)

Studies of the persistent current relaxation of $YBa_2Cu_3O_{7-\delta}$ ring-shaped thin films as a function of oxygen concentration (with 24 increments in δ every ~0.021, over a range between 0.03 and 0.55) allowed us to construct the (μ, δ) phase diagram where the exponent μ characterizes the pinning ability and the nature of the vortex structure. The reduction of the hole-doping level (an increase in δ) transforms the vortex structure from quasi-lattice into a glass and subsequently into a pinned liquid phase. These vortex phases self-organize and produce relaxation plateaus in regions between steplike changes in the dependence of relaxation kinetics on hole doping.

DOI: 10.1103/PhysRevB.79.172504 PACS number(s): 74.25.Ha, 74.25.Qt, 74.25.Sv, 74.62.Dh

I. INTRODUCTION

Vortex matter in high-temperature superconductors including the interaction of magnetic vortices with impurities, as well as the response of these vortices to external magnetic fields, has been intensively investigated, both theoretically and experimentally.[1–5] In defect-free superconductors an electric current flowing inside the sample induces vortex motion, causing resistance and subsequent dissipation of the supercurrent.[2] Pinning the vortices by lattice defects hinders this dissipative process, deforms the vortex structure, and increases the critical currents. Studies of the $(H\text{-}T)$ phase diagram of the vortex structure have been conducted using the (equilibrium) thermodynamical approach, i.e., by probing the response of the vortex structure to external magnetic fields (H) applied at different temperatures below T_c.[4–6] It has been shown by equilibrium magnetization and specific heat measurements[4] that high magnetic fields can melt the vortex lattice. These measurements have identified lattice-, glass-, and liquid-vortex phases, at some fixed defect-concentration levels. However, the nature of the vortex phase diagram, and especially the significance of scaling exponents, remains controversial. Recently it was suggested that a good description of the phase diagram would utilize scaling exponents from smectic liquid-crystalline phases which produces resistivity-electric-field exponents that vary by a factor of 15.[7]

The response of the vortex structure to successive infinitesimal disorder levels in the $J \ll J_c$ limit[3] is of considerable interest to theorists who study vortex pinning in superconductors since it is one of the key elements that determines the statistical mechanics and the dynamics of the vortex system. Although there were many studies of vortex creep in granular structures in the early 1990s, Blatter *et al.*[3] suggested in 1994 that "a systematic experimental study of the correlation between oxygen-defect concentration and the critical current density [in single crystals] would be highly desirable."

Oxygen vacancies are an important example of intrinsic disorder and can be created in a superconductor by annealing, for example. The vacancies change the hole-doping level of the material, which in turn determines the superconducting order parameter of the sample and, therefore, its properties such as the transition temperature (T_c), the superfluid density, as well as the vortex structure. This implies that one way to investigate the intrinsic disorder-induced vortex structure in bulk superconductors is to study the time evolution, i.e., relaxation of the persistent current generated in the superconductor in samples with different oxygen-defect concentration.[3] The nature of the vortex structures and their pinning in the presence of the persistent current can be inferred from the value of the exponent μ, a parameter in the scaling relation[3,8,9] between the effective energy barrier against vortex motion U_{eff} and the persistent current density J, i.e., $U_{\text{eff}}(J) \propto (J_c/J)^{\mu}$, where J_c is the critical current density. Furthermore, the critical current-density ratio in the as-grown and annealed samples can be used as an indicator of the strength of the disorder.[3]

In this Brief Report, we report studies of the evolution of the vortex structure inferred from measurements of the persistent current relaxations of 24 different oxygen contents (with δ changing from 0.03 to 0.55 in steps of about 0.021) of the same $YBa_2Cu_3O_{7-\delta}$ (YBCO) ring-shaped epitaxial films. This type of measurement is equivalent to that of the remanent magnetization trapped in a superconductor at a zero external magnetic field. This has enabled us to map out the phase diagram of the vortex structure (the vortex-structure exponent μ versus δ) in $YBa_2Cu_3O_{7-\delta}$. We found that an increase in disorder (increase in δ) leads to the transformation of the vortex quasi-lattice into a glass and subsequently into a pinned liquid. These vortex phases self-organize and produce relaxation plateaus in regions between steplike changes in the dependence of the relaxation kinetics on the hole doping, showing an important correlation between the vortex structure and the hole-doping level in $YBa_2Cu_3O_{7-\delta}$ films.

II. EXPERIMENTAL DETAILS

The relaxation of the persistent current was measured on ring-shaped samples in order to provide the information on both the vortex-motion-induced persistent current decay and the persistent current density. The experiments were done on $YBa_2Cu_3O_{7-\delta}$ (slightly overdoped with $T_c \approx 88$ K) ring-shaped 0.2-μm-thick films of inner and outer diameters 4.6 and 7.2 mm, respectively. The films were deposited on a $\langle 100 \rangle$-oriented $LaAlO_3$ substrate using the rf-magnetron-

sputtering technique. X-ray diffraction revealed highly epitaxial films. A persistent circulating supercurrent was induced in the ring by cooling it in a zero field to the temperature of interest below T_c, then applying an external magnetic field along the ring's axis, and subsequently reducing it to zero. The axial profile of the magnetic self-field $B_z(r)$ of the persistent current was then measured across the ring with a traveling Hall sensor positioned in air at room temperature at a distance of 2.5 mm above the sample surface.[10] The magnitude of the current was obtained from $B_z(r)$ using the Biot-Savart's law. The critical value of the persistent current is reached when $B_z(r)$ becomes independent of the applied magnetic field. This is a contactless technique which allows one to distinguish between the magnetic field due to the circulating persistent current and that due to the trapped vortices in the ring's bulk.[11]

In our experiments, we gradually increased δ and reduced the hole-doping p, i.e., the number of holes per Cu atom of the CuO_2 planes, by annealing the film in flowing argon at a temperature of 175 °C. This was done a number of times in steps of a few hours each so that T_c was reduced from 88 down to 55.5 K. The relatively low annealing temperature ensured the reduction in the hole doping by removing oxygen from YBCO without affecting extended defects, such as dislocations and grain boundaries. The measurements of the persistent current density and its time dependence up to 10^4 s were performed at temperatures between 10 and T_c in 5 K steps, after each annealing step. The ratio (J_1^o/J_1), where J_1^o and J_1 are the current densities measured after 1 s at 10 K in the as-grown and annealed films, respectively, has been used as an indicator of the disorder level in the material.[3] (J_1^o/J_1) increases with an increasing annealing time.

III. RESULTS AND DISCUSSION

Figure 1(a) shows selected $J(T,t)$ curves for the YBCO thin-film ring at different levels of disorder J_1^o/J_1. The length of the vertical traces of J at each temperature in Fig. 1(a) indicates the decay of J at a specific disorder level over a time interval between 1 and 3600 s. The time dependence of the persistent current density $J(t)$ at different temperatures was used to calculate the dependence of the normalized decay rate (the creep rate) $S=-d\ln(J)/d\ln(t)$ on temperature, which is a result of the dissipative motion of the vortices over an effective energy barrier U_{eff}. Figure 1(b) shows selected curves of $S(T)$ demonstrating the change in $S(T)$ with an increasing disorder. Typical dependence of S on the disorder level is shown in Fig. 1(c) for a constant temperature of 20 K. The increase in S with the disorder indicates an ongoing softening process of the vortex structure and the resulting creep of vortices.

In order to obtain the information about the vortex structure at different levels of disorder, the Maley scheme[8] could be applied to calculate the critical exponent μ in the dependence of the energy barrier on the current density $U_{\text{eff}}(J) \propto (J_c/J)^{\mu}$. The decay rate of the persistent current dJ/dt from the critical level in a zero external magnetic field (which is equivalent to the decay rate of the remanent magnetization) depends on the energy barrier $U(J)$ as $dJ/dt \propto -J_o \exp[-U(J)/k_BT]$ where J_o is the current density close to the critical current value.[12] The energy barrier could then be extracted from this equation as $U(J,T) \simeq -k_BT\{\ln|(dJ/dt)/J_o| - C\}$ where k_B is the Boltzmann constant. C is a constant that can be adjusted in order to ensure that $U(J)$ is a continuous function of J at low temperatures.[8] In order to find U, the decay rate dJ/dt was first calculated from the measured decay of the current density $J(t)$ over a time interval of 60–3600 s. J_o was selected as the experimentally accessible current density recorded 1 s after the critical state was established in the ring. Then a factor $-k_BT\ln[|(dJ/dt)/J_o|]$ in $U(J,T)$ was plotted as a function of J [see Fig. 2(a)]. Multiple segments seen in this plot were measured at different temperatures between 10 K and T_c. By choosing an appropriate value of a constant C ($\approx$21.5, for all doping levels $C=20\pm3$), it was possible to align these segments at low temperature [see Fig. 2(b)]. Subsequent division of $U(J,T)$ by a thermal factor $g(T) \leq 1$ (Refs. 9 and 12) gave a piecewise continuity of all the segments [see Fig. 2(c)]. The thermal factor $g(T)$ was found to be almost the same irrespective of the doping level [see Fig. 2(d)]. The resulting effective energy barrier $U_{\text{eff}}(J)=U(J,T)/g(T) \propto (J_c/J)^{\mu}$ has been used to calculate the critical exponent μ.

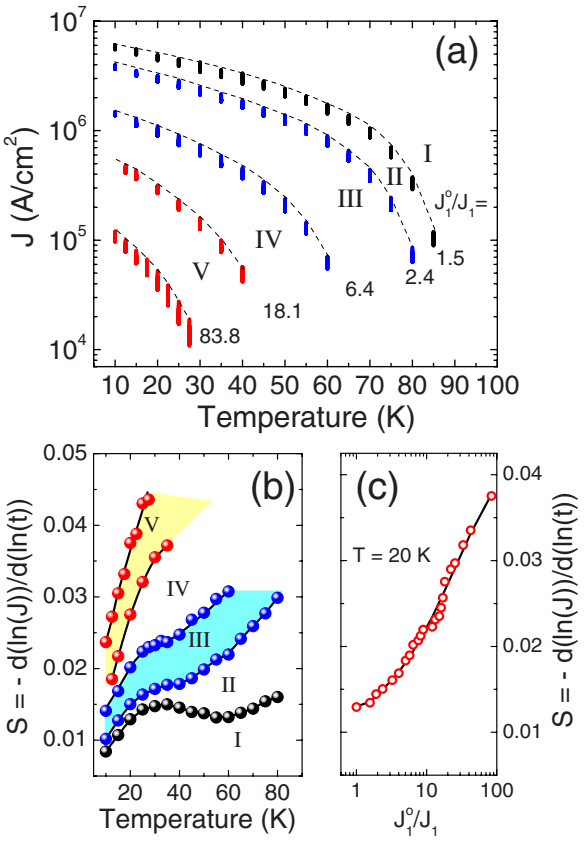

FIG. 1. (Color online) (a) Temperature dependence of the persistent current density J at selected levels of disorder indicated by the ratio (J_1^o/J_1) (thin-dashed lines). The vertical traces show the dependence of $J(T,t)$ on time. (b) Temperature dependence of the normalized decay rate S of the persistent current density corresponding to the same disorder levels as in (a). Regions I–V are explained in the text. (c) S as a function of (J_1^o/J_1) for a constant temperature of 20 K. (The lines are guides to the eyes).

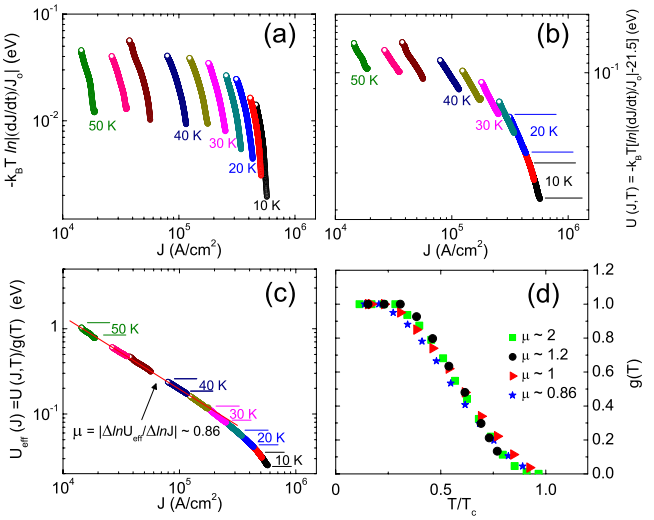

FIG. 2. (Color online) (a) Plot of the expression $-k_BT\ln|(dJ/dt)/J_o|$ as a function of the current density J which displays vertically shifted segments (see text). (b) Plot of $U(J,T) \simeq -k_BT[\ln|(dJ/dt)/J_o| - 21.5]$ as a function of J, for a constant C adjusted to 21.5 which aligns the low-temperature segments. (c) The effective energy barrier $U_{\rm eff}(J) = U(J,T)/g(T) \propto (J_c/J)^{\mu}$ versus J. (d) Thermal factors $g(T)$ corresponding to several different doping levels and $\mu \sim 2$, 1.2, 1, and 0.86.

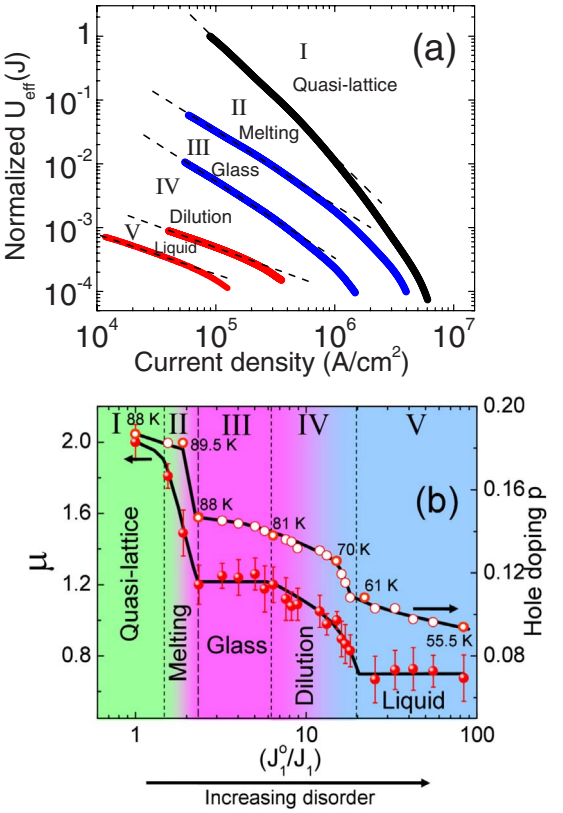

FIG. 3. (Color online) (a) Maley's plots showing the dependence of $U_{\rm eff}(J)$ (normalized to that of the as-grown sample at $J \sim 10^5$ A/cm^2) on the current density for different disorder levels. The dashed lines indicate the regions of J for which μ was calculated (see text). (b) Evolution of the vortex structure represented by the change of the critical exponent μ (solid spheres) and hole-doping number p (open circles) as a function of disorder J_1^o/J_1 in YBCO. Three different vortex phases, as well as two transition stages (melting and dilution), are shown. Temperatures mark T_c's for selected hole-doping numbers. Solid lines are guides to the eyes.

For each value of the doping level, the value of μ was calculated from the dependence $U_{\rm eff} \propto (J_c/J)^{\mu}$ for current densities less than $0.7J_c$. This range of J was selected in order to ensure that the Lorentz force on the vortex structure is relatively low and the above equation is satisfied.[3,12,13]

Selected curves of $U_{\rm eff}(J) = U(J,T)/g(T)$ (the Maley plots) labeled I–V are shown in Fig. 3(a) for different levels of disorder. The analysis of the persistent current relaxations enabled us to construct the phase diagram (δ,μ) of the vortex structure shown in Fig. 3(b). It shows the evolution of the vortex structure and the hole-doping level p as a function of an increasing disorder level. In order to calculate the value of the hole doping of the disordered film, we used the dependence of p on T_c which was measured for YBCO single crystals.[14] Vortex phases in this diagram are identified by the value of the critical exponent (the vortex-structure order parameter) μ,[3,13] obtained as described above. Vortices in the as-grown film are expected to be arranged in a quasi-long-range ordered lattice;[15] therefore, we have assigned this state, and hence region I, in Fig. 3(b) accordingly (the Bragg "lattice" phase).

As mentioned in the introduction, it is well known that an increasing magnetic field can produce changes in the vortex phase.[4] Interestingly, we observed that even in the absence of an applied magnetic field, the original vortex structure in the film can be subsequently deformed/melted upon increasing the intrinsic lattice disorder in the sample. In particular, Fig. 3(b) shows that μ strongly depends on the disorder level in YBCO film. We measured μ in two films with similar results obtained. Starting with the vortex quasi-lattice in the as-grown film with $\mu_c \sim 2.0 \pm 0.1$ (region I), a small change in the disorder level (J_1^o/J_1) causes a dramatic drop (region II) in the critical exponent down to $\mu_g \sim 1.22 \pm 0.04$. The latter value is consistent with $\mu \sim 1$ of the glass phase observed in YBCO.[16] We attribute this drop to a melting transition of the vortex-quasi-lattice phase into a glasslike phase (region III) which has shorter-range order. The glass phase persists over a wider range of intrinsic disorder than the quasilattice phase. As the level of disorder is increased further, the value of μ drops monotonically (region IV) until it eventually plateaus at a sublinear value of $\mu_l \sim 0.71 \pm 0.03$ (region V). We assign region V to a pinned liquid phase and therefore, in region IV, a dilution process is taking place where both vortex glass and liquid phases coexist. The assignment of $\mu_l \sim 0.71$ to a liquid phase (region V) is made because of comparisons with theory, such as the calculations from a Gibbsian droplet nucleation model of bulging elastic vortices.[3] Similar values of $\mu_l \sim 0.77$ have been reported for magnetic relaxation in a vortex liquid in $HgBa_2Ca_2Cu_3O_{8+\delta}$ thin films.[17]

An increase in the concentration of oxygen vacancies reduces the coupling between the CuO_2 planes[18] and leads to a "monotonic" increase in the anisotropy of YBCO.[19] Hence the changes of anisotropy cannot be correlated with the observed plateaus in μ. Moreover, in the range of T_c's between 86.8 and 92 K (for $\delta \leq 0.11$) where dramatic changes in μ

are observed [see regions I–III in Fig. 3(b)], the changes in anisotropy are very small.[20]

Upon reoxygenating the film, μ recovers to a value of 1.98 ± 0.11 which is close to that of $\sim 2.0 \pm 0.1$ found in the as-grown sample prior to deoxygenation. This indicates that our observations are reversible. The results for μ_c, μ_g, and μ_l imply that an important correlation exists between the vortex structure and the hole doping of the CuO_2 planes. The hole doping decreases gradually with an increasing disorder level in a steplike manner. The steps occur at the boundaries between regions II and III, and between regions IV and V, i.e., at the onsets of the formation of the vortex-glass and vortex-liquid phases. Power-law scaling (characteristic of self-organized structures[21]) is not predicted by recent formal theories based on collective pinning by randomly distributed dopants[22] but it is predicted with a sublinear scaling exponent of the liquid phase ($\mu_l \sim 0.71$) by nucleation of vortex bulges[3] which gives $\mu_l = (6-d)/4$ or 0.75 for $d=3$, i.e., three-dimensional vortices (with kinks). So far nucleation theory has no explanation for the superlinear exponents reported here for the strongly correlated (self-organized) lattice ($\mu_c \sim 2$) and glass ($\mu_g \sim 1.22$) phases. The wide region corresponding to the glass phase, with its constant μ_g, is not predicted by most theories but a similarly wide region has been observed in the phase diagrams of network glasses, where it was called the intermediate phase.[23,24] This self-organized phase has special elastic and thermal properties[25] analogous to the creep of glassy vortex arrays in high-temperature superconductors.

IV. CONCLUSION

In summary, we found that the evolution of the vortex structure of $YBa_2Cu_3O_{7-\delta}$ correlates with the changes in the hole-doping level in the CuO_2 planes. As δ increases, the collective lattice self-organization of the as-grown sample decreases, leading to the formation of vortex-glass and vortex-liquid phases. These vortex phases form in regions between steplike changes in the dependence of the hole doping on disorder, corresponding to mixed phases. The fundamental results of our studies should stimulate further development and renewed interest of theories of the vortex structure and its response to intrinsic lattice disorder and/or a hole-doping level in high-temperature superconductors.

ACKNOWLEDGMENT

This work was supported by the Natural Sciences and Engineering Research Council of Canada.

*amansour@phys.ualberta.ca
†jung@phys.ualberta.ca

[1] A. A. Abrikosov, Rev. Mod. Phys. **76**, 975 (2004).
[2] Y. B. Kim, C. F. Hempstead, and A. R. Strnad, Phys. Rev. **139**, A1163 (1965).
[3] G. Blatter, M. V. Feigel'man, V. B. Geshkenbein, A. I. Larkin, and V. M. Vinokur, Rev. Mod. Phys. **66**, 1125 (1994).
[4] F. Bouquet *et al.*, Nature (London) **411**, 448 (2001).
[5] J. Kierfeld and V. Vinokur, Phys. Rev. B **69**, 024501 (2004); **61**, R14928 (2000).
[6] H. Beidenkopf *et al.*, Phys. Rev. Lett. **95**, 257004 (2005).
[7] S. A. Baily *et al.*, Phys. Rev. Lett. **100**, 027004 (2008).
[8] M. P. Maley, J. O. Willis, H. Lessure, and M. E. McHenry, Phys. Rev. B **42**, 2639 (1990).
[9] J. R. Thompson, L. Krusin–Elbaum, L. Civale, G. Blatter, and C. Feild, Phys. Rev. Lett. **78**, 3181 (1997).
[10] A. I. Mansour *et al.*, Appl. Phys. Lett. **90**, 162511 (2007); A. I. Mansour, M. M. Saber, K. H. Chow, and J. Jung, *ibid.* **93**, 142509 (2008).
[11] H. Darhmaoui, J. Jung, J. Talvacchio, M. A.-K. Mohamed, and L. Friedrich, Phys. Rev. B **53**, 12330 (1996).
[12] M. Nideröst, A. Suter, P. Visani, A. C. Mota, and G. Blatter, Phys. Rev. B **53**, 9286 (1996).
[13] C. J. van der Beek *et al.*, Physica C **195**, 307 (1992).
[14] R. Liang, D. A. Bonn, and W. N. Hardy, Phys. Rev. B **73**, 180505(R) (2006).
[15] R. H. Koch *et al.*, Phys. Rev. Lett. **63**, 1511 (1989).
[16] A. P. Malozemoff and M. P. A. Fisher, Phys. Rev. B **42**, 6784 (1990).
[17] M. H. Kim, S. I. Lee, M. S. Kim, and W. N. Kang, Supercond. Sci. Technol. **18**, 835 (2005).
[18] W. Lang, W. Gob, W. Kula, and R. Sobolewski, Z. Phys. B: Condens. Matter **98**, 453 (1995).
[19] T. R. Chien *et al.*, Physica C **229**, 273 (1994); M. Putti *et al.*, *ibid.* **314**, 247 (1999).
[20] J. G. Ossandon *et al.*, Phys. Rev. B **45**, 12534 (1992); **46**, 3050 (1992).
[21] V. M. Vinokur, M. V. Feigel'man, and V. B. Geshkenbein, Phys. Rev. Lett. **67**, 915 (1991).
[22] B. Rosenstein and V. Zhuravlev, Phys. Rev. B **76**, 014507 (2007).
[23] K. Rompicharla *et al.*, J. Phys.: Condens. Matter **20**, 202101 (2008).
[24] J. C. Phillips, Proc. Natl. Acad. Sci. U.S.A. **105**, 9917 (2008); Phys. Rev. B **75**, 214503 (2007).
[25] S. Chakravarty, D. G. Georgiev, P. Boolchand, and M. Micoulaut, J. Phys.: Condens. Matter **17**, L1 (2005).